PNAS RESEARCH ARTICLE | BIOCHEMISTRY

Engineering peroxisomal biosynthetic pathways for maximization of triterpene production in *Yarrowia lipolytica*

Yongshuo Ma[a], Yi Shang[b,c,1], and Gregory Stephanopoulos[a,1]

Contributed by Gregory Stephanopoulos; received August 25, 2023; accepted December 20, 2023; reviewed by Mattheos A. Koffas and Jens Nielsen

Constructing efficient cell factories for product synthesis is frequently hampered by competing pathways and/or insufficient precursor supply. This is particularly evident in the case of triterpenoid biosynthesis in *Yarrowia lipolytica*, where squalene biosynthesis is tightly coupled to cytosolic biosynthesis of sterols essential for cell viability. Here, we addressed this problem by reconstructing the complete squalene biosynthetic pathway, starting from acetyl-CoA, in the peroxisome, thus harnessing peroxisomal acetyl-CoA pool and sequestering squalene synthesis in this organelle from competing cytosolic reactions. This strategy led to increasing the squalene levels by 1,300-fold relatively to native cytosolic synthesis. Subsequent enhancement of the peroxisomal acetyl-CoA supply by two independent approaches, 1) converting cellular lipid pool to peroxisomal acetyl-CoA and 2) establishing an orthogonal acetyl-CoA shortcut from CO_2-derived acetate in the peroxisome, further significantly improved local squalene accumulation. Using these approaches, we constructed squalene-producing strains capable of yielding 32.8 g/L from glucose, and 31.6 g/L from acetate by employing a cofeeding strategy, in bioreactor fermentations. Our findings provide a feasible strategy for protecting intermediate metabolites that can be claimed by multiple reactions by engineering peroxisomes in *Y. lipolytica* as microfactories for the production of such intermediates and in particular acetyl-CoA-derived metabolites.

triterpenoids | metabolic engineering | peroxisome | orthogonal pathway | acetate metabolism

Significance

It is often challenging to redirect metabolic fluxes toward heterologous pathways to synthesize desirable products when competing for common precursors with native metabolism critical for cell viability. An example is the synthesis of triterpenoids in *Yarrowia lipolytica,* whose precursor squalene is coupling \to cytosolic sterol biosynthesis. To overcome this challenge, we engineered the peroxisomes of *Y. lipolytica* for squalene biosynthesis, thus isolating it from competing cytosolic reactions. Additional enhancement of the acetyl-CoA precursor supply in the peroxisome through engineering cellular lipid metabolism or acetate metabolism further improved cellular fitness and squalene biosynthesis. This study provides a method for squalene production but also unlocks the potential of peroxisomes in *Y. lipolytica* for the production of a wide range of acetyl-CoA-derived chemicals.

Engineering microorganisms for the production of high-value compounds from renewable feedstocks is a promising alternative to plant sourcing or fossil-dependent production (1–4). However, metabolic engineering efforts to achieve economically viable titers and productivities are frequently hampered by native competing pathways and metabolic cross talk (3). This is because host metabolic networks have evolved tight regulatory systems to maintain metabolic homeostasis, which make it particularly challenging to redirect metabolic fluxes toward product synthesis that competes with native metabolism (5). Although blocking competing pathways by inactivating competing genes (6), or utilizing inducible (7, 8) and weaker promoters (9) have worked in certain cases, inactivating endogenous pathways that are essential for cell growth presents special challenges and more effective approaches are needed to funnel metabolic fluxes to target products. An alternative solution would be to reduce the connectivity of the pathway of interest with the competing native metabolism, thus making the product pathway orthogonal to the host metabolic network (10, 11). Reprogramming cellular metabolism and establishing an orthogonal product route would decouple production from native metabolism and, as such, be advantageous for improved pathway control and performance.

A characteristic case of the above pathway competition is the synthesis of triterpenoids in yeast, where biosynthesis of their precursors is tightly coupled with sterol biosynthesis. Triterpenoids are one of the largest and most structurally diverse families of natural products, and many have been shown to possess valuable properties for use in the food industry, cosmetic production, and pharmacology (12, 13). Among these, squalene is a linear triterpene oil widely used as a dietary supplement, moisturizer, and antitumor agent in pharmaceutical, health care, and cosmetic industries (14). In particular, squalene has been employed as an essential component of nanoemulsion vaccine adjuvants in seasonal influenza and COVID-19 vaccines (15). Furthermore, squalene is a key precursor for the synthesis of all triterpenoids and sterols in nature (12). Currently, it is commercially sourced mainly from shark liver oil and plant seeds (16). Due to a sizeable and rapidly expanding world market, developing alternative natural sources at reasonable cost has become an urgent priority. In prior research, manipulations of central carbon metabolism and the MVA pathway, downregulation of competing pathways, and cofactor regeneration have yielded encouraging results for squalene production in terms of improved productivity in several microbial strains (14), including *Saccharomyces cerevisiae* (9, 17–24), *Escherichia*

Author contributions: Y.M. and G.S. designed research; Y.M. performed research; Y.M. and Y.S. analyzed data; and Y.M. and G.S. wrote the paper.

Reviewers: M.A.K., Rensselaer Polytechnic Institute; and J.N., BioInnovation Institute.

Competing interest statement: Y.M. and G.S. are coinventors in a patent application (Serial No.: 63/481,957) describing the squalene production using the strategies reported here.

Copyright © 2024 the Author(s). Published by PNAS. This article is distributed under Creative Commons Attribution-NonCommercial-NoDerivatives License 4.0 (CC BY-NC-ND).

[1]To whom correspondence may be addressed. Email: shangyi@ynnu.edu.cn or gregstep@mit.edu.

This article contains supporting information online at https://www.pnas.org/lookup/suppl/doi:10.1073/pnas.2314798121/-/DCSupplemental.

Published January 23, 2024.

Downloaded from https://www.pnas.org by MASARYK UNIVERZITNIHO KAMPUSU on November 3, 2024 from IP address 147.251.22.2.

coli (25–28), and *Yarrowia lipolytica* (29–33). However, production titers and yields achieved are still low for cost effective production, which remains a major challenge.

In this study, using the oleaginous yeast *Y. lipolytica*, we explore the possibility of expressing an orthogonal metabolic network in the peroxisome to circumvent metabolic competitions for triterpene synthesis. We also investigate two independent strategies for effectively enhancing the supply of the key precursor acetyl-CoA in the peroxisome for triterpene production. In yeast, squalene synthesis occurs in the cytosol and is tightly coupled to the biosynthesis of sterol that is essential for cell growth and viability. This is a very strong metabolic coupling, which creates a major challenge for constructing robust squalene-producing strains with high productivity. To isolate squalene synthesis, we constructed an orthogonal pathway in the peroxisome by introducing the complete squalene biosynthetic pathway starting from acetyl-CoA, in which the mevalonate (MVA) pathway is assembled to harvest peroxisomal acetyl-CoA pool. The peroxisome efficiently insulates locally formed squalene from competing cytosolic reactions, thus circumventing the need to bypass intricate regulatory mechanisms evolved in order to maintain sterol synthesis in the cytosol. However, sequestration of the squalene pathway in the peroxisome depletes the native supply of the precursor acetyl-CoA in the peroxisome necessitating the introduction of additional acetyl-CoA supply routes. To this end, our first strategy was to engineer pathways for the biosynthesis, hydrolysis, and degradation of lipids to achieve conversion of accumulated lipids to peroxisomal acetyl-CoA pool. This approach yielded strains capable of producing 32.8 g/L squalene from glucose with a 0.15 g/L/h productivity in bioreactor fermentations. Alternatively, in the second approach, similar production levels of squalene were obtained by establishing an orthogonal acetyl-CoA shortcut in the peroxisome that harnessed acetate-utilizing pathway, yielding 31.6 g/L squalene from acetate with a 0.14 g/L/h productivity in the bioreactor employing a glucose cofeeding strategy. Overall, our findings illustrate a blueprint for efficient production of acetyl-CoA-derived chemicals in *Y. lipolytica*.

Results

Identifying Rate-Limiting Steps in the Squalene Biosynthetic Pathway. In yeast, squalene is only synthesized as an intermediate in the sterol biosynthetic pathway (Fig. 1*A*), which is essential for cell growth and viability. The cytosolic farnesyl pyrophosphate synthetase (ERG20) functions as a bifunctional synthase that sequentially catalyzes the condensation of isopentenyl diphosphate

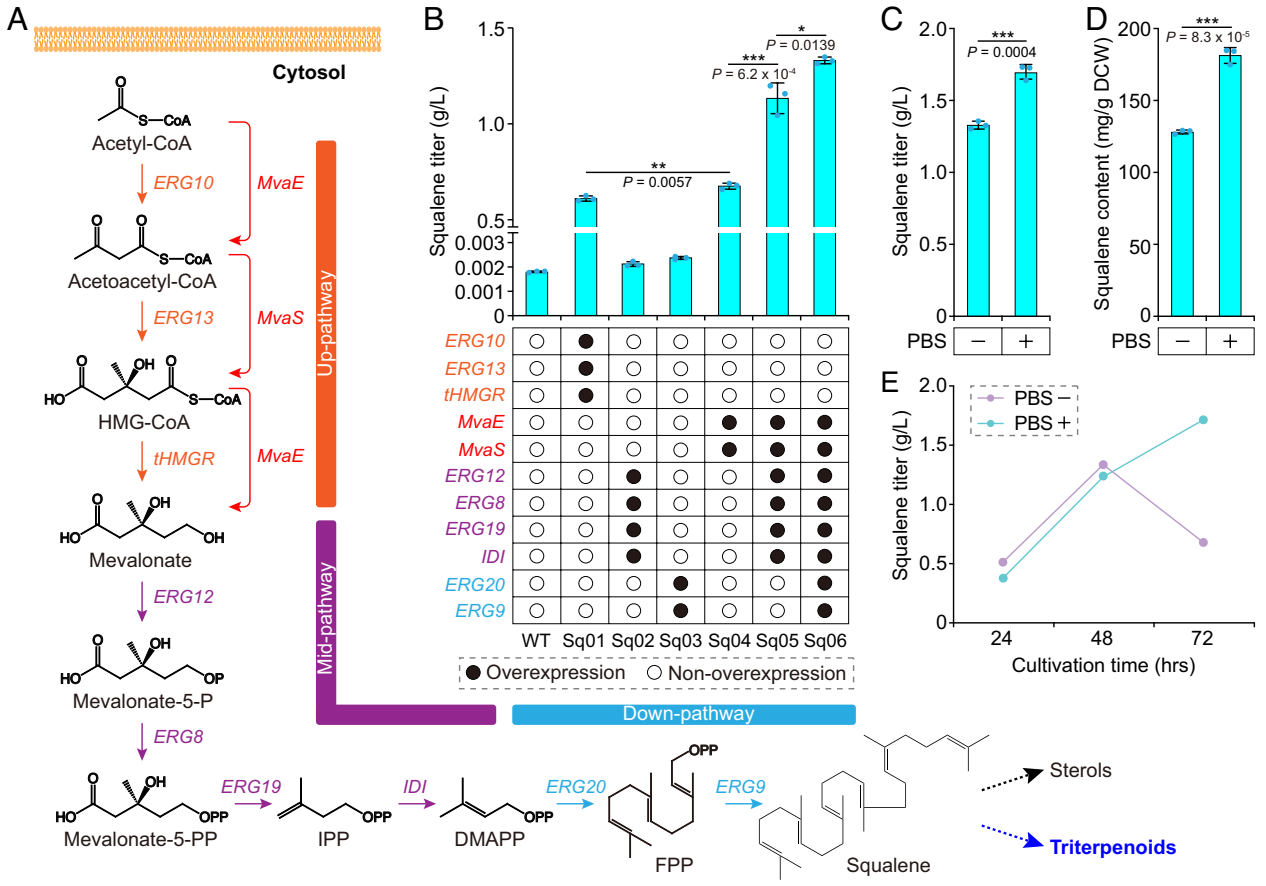

Fig. 1. Engineering the cytosolic metabolic pathway for squalene production in *Y. lipolytica*. (*A*) Schematic view of the metabolic pathway for squalene biosynthesis in the cytosol. The biosynthetic pathway of squalene starting from acetyl-CoA was divided into three modules: up-pathway (shown in red), mid-pathway (shown in purple), and down-pathway (shown in blue). ERG10, acetyl-CoA acetyltransferase. ERG13, 3-hydroxy-3-methylglutary-CoA (HMG-CoA) synthase. tHMGR, truncated HMG-CoA reductase. ERG12, mevalonate kinase. ERG8, phosphomevalonate kinase. ERG19, mevalonate pyrophosphate decarboxylase. IDI, IPP:DMAPP isomerase. ERG20, farnesyl pyrophosphate synthetase. ERG1, squalene synthase. MvaE and MvaS, from *Enterococcus faecalis*. IPP, isopentenyl diphosphate. DMAPP, dimethylallyl diphosphate. FPP, farnesyl pyrophosphate. (*B*) Each module was overexpressed in *Y. lipolytica*, individually and in combination. Squalene titers were measured after 48 h of fermentation in YPD media. (*C* and *D*) Squalene titers (*C*) and intracellular content (*D*) were significantly enhanced when YPD media were supplemented with 0.2 M PBS. Samples in media without supplemented PBS were measured at 48-h cultivation, whereas samples in supplemented PBS media were measured at 72-h cultivation. (*E*) Fermentation time-course profiles indicated that PBS-added fermentation reached the highest squalene titers at 72-h cultivation, yet, at 48 h in the PBS-unconditioned fermentation. Statistical significance was tested using the two-sided Student's *t* test; $*P < 0.05$, $**P < 0.01$, and $***P < 0.001$. All data are represented as mean ± SD of three biologically independent experiments.

Downloaded from https://www.pnas.org by MASARYK UNIVERZITNIHO KAMPUSU on November 3, 2024 from IP address 147.251.22.2.

(IPP) and dimethylallyl pyrophosphate (DMAPP), generated through the MVA pathway, to form farnesyl diphosphate (FPP). The latter is subsequently converted by ERG9, encoding squalene synthase, to squalene (Fig. 1*A*). Due to the tightly regulated and balanced sterol synthesis pathway, the content of native synthesized squalene in wild-type *Y. lipolytica* Po1f is extremely low, only 1.8 mg/L (Fig. 1*B*). To construct the cell factories for squalene overproduction, we first set out to determine possible rate-limiting steps in the squalene biosynthetic pathway, which would identify targets for further optimization. Given the mevalonate and IPP/DMAPP in the MVA pathway as the key precursors for terpene biosynthesis, the squalene biosynthetic pathway starting from acetyl-CoA was divided into three modules: up-pathway (upstream of MVA containing ERG10, ERG13, and tHMGR), mid-pathway (downstream of MVA containing ERG12, ERG8, ERG19, and IDI), and down-pathway (squalene forming route containing ERG20 and ERG9) (Fig. 1*A*). In addition, we also investigated the capacity of the heterologous *Enterococcus faecalis* MvaE and MvaS enzymes which catalyze the first three steps in the MVA pathway (corresponding to the reactions catalyzed by ERG10, ERG13, and tHMGR proteins) (Fig. 1*A*), owing to their good performance in *S. cerevisiae* (34, 35).

Each module was respectively overexpressed in *Y. lipolytica* Po1f-T-L strain, a variant of Po1f with *TRP1* and *LYS5* disruption (36) (*SI Appendix*, Fig. S1), and their capacity for squalene production were assessed. Upregulation of the up-pathway revealed that the enzymes ERG10, ERG13, and tHMGR are the main bottlenecks in the pathway, as their combined overexpression led to 344-fold increase (a titer of 0.62 g/L) in squalene production relative to its parent strain (Sq01 vs. WT, Fig. 1*B*). In contrast, the effect of mid- or down-pathway overexpression on squalene production was very limited (only 1.2-fold or 1.3-fold increase over the parent strain, Sq02 or Sq03 vs. WT, Fig. 1*B*), suggesting that the catalyzation of the corresponding enzymes is not limiting step. Intriguingly, strain harboring heterologous *MvaE* and *MvaS* produced a titer of 0.69 g/L squalene and significantly increased by 11.3% squalene production compared to that of overexpressing endogenous up-pathway enzymes (ERG10, ERG13, and tHMGR) (Sq04 vs. Sq01, Fig. 1*B*). Thus, the MvaE and MvaS pair were used as alternative shortcut of the up-pathway in all subsequent studies. When the expression levels of both up- and mid-pathway were up-regulated together or the entire squalene synthetic pathway was overexpressed, an additional 1.7-fold or 2.0-fold increase in squalene production was observed (Sq05 or Sq06 vs. Sq04, Fig. 1*B*), ultimately reaching a titer of 1.34 g/L in Sq06, possibly due to the improved availability of pathway intermediates.

These results suggest that for the most part, the upregulation of the squalene synthetic pathway in the cytoplasm functions efficiently for squalene biosynthesis (744-fold increase in Sq06 vs. WT, Fig. 1*B*). The most crucial step is the up-pathway, which competes for the common precursor acetyl-CoA with de novo lipid formation in *Y. lipolytica*. On the other hand, while individual mid- and down-pathway upregulation barely affected squalene production in the absence of up-pathway overexpression, their roles appear to be dependent on the strength of the up-pathway, as the overexpression of the up-pathway increases the amounts of MVA pool, which, in turn, requires high-level of expression of the downstream enzymes to be fully harvested.

Interestingly, we accidentally found that the squalene production in terms of both titer (1.71 g/L, Fig. 1*C*) and cellular content (182.8 mg/g DCW, Fig. 1*D*) was significantly increased by 27% and 41%, respectively, when YPD media were supplemented with 0.2 M phosphoric buffer solution (PBS, pH 6.0). This can be attributed to the pH control in the media conditioned with PBS relatively to media not containing PBS (*SI Appendix*, Fig. S2). The latter allowed significant pH variation, which may negatively affect cell physiology, including the permeability of cell membrane and nutrient transport (37). Furthermore, the pH-controlled fermentation process prolonged the phase of squalene biosynthesis and reached the highest titer at 72-h cultivation, whereas the optimal production in the pH-uncontrolled fermentation was observed at 48-h cultivation, and decreased significantly afterward (Fig. 1*E*). Thus, the PBS-conditioned media were used in all subsequent studies.

Establishing an Orthogonal Biosynthetic Route for Squalene in the Peroxisome. While up-regulating cytosolic squalene synthesis pathway improved squalene production, the strong competition by cytosolic sterol synthesis optimized through evolution makes it particularly challenging for large squalene accumulation in the cytosol. Therefore, further efforts focused on sequestering squalene from its competing pathway and preventing its conversion to by-products. Eukaryotic cells have evolved solutions to similar challenges by confining metabolic pathways within intracellular organelles to streamline cascade reactions and prevent intermediates from competing pathways (35). Inspired by this, we hypothesized that sequestering biosynthetic pathway for squalene synthesis in a yeast organelle would prevent it diversion from competing cytosolic pathways. Here, we focused on the peroxisomes because, a) peroxisomes are not essential for cell viability (38), which allows them to be extensively engineered without impacting yeast fitness; b) they are the places where fatty acid degradation occurs, generating acetyl-CoA pool that can be utilized by a heterologous MVA pathway for squalene synthesis; and c) peroxisomes also serve as storage compartments for lipophilic compounds (9), which would provide space for intracellular squalene accumulation. The above considerations underline the potential of advantageously repurposing peroxisomal pathways for efficient squalene synthesis (Fig. 2*A*).

To evaluate the suitability of the peroxisome in *Y. lipolytica* for squalene production, we first set out to direct the down-pathway containing ERG20 and ERG9 to the peroxisome by fusing a peroxisomal targeting signal SKL at C-terminal (Fig. 2*A*). Squalene production drastically improved by 6.3-fold, compared to that of their cytosolic overexpression (Sq07 vs. Sq03, Fig. 2*B*). In addition, a higher biomass was observed in strain Sq03 relatively to Sq07 (*SI Appendix*, Fig. S3), which can be possibly attributed to more squalene channeled into the sterol pathway in Sq03, thereby promoting cell growth. These results support the initial hypothesis that the peroxisome can serve as a barrier and insulate locally formed squalene from cytosolic sterol synthesis. The data also suggested that precursors IPP and DMAPP generated by the cytosolic MVA pathway could be translocated into the peroxisome from the cytosol for squalene synthesis.

To expand on these findings, we next investigated the possibility to harvest the available pool of peroxisomal acetyl-CoA for squalene synthesis in this organelle. To this end, we sequentially introduced the enzymes involving the MVA pathway into the peroxisome. In the presence of ERG20 and ERG9, sequential addition of the mid-pathway (ERG12, ERG8, ERG19, and IDI) in the peroxisome led to additional 3.8-fold increase of squalene production (Sq09 vs. Sq07, Fig. 2*B*), while their cytosolic overexpression only had a minor impact on squalene production (Sq08 vs. Sq03, Fig. 2*B*). When the complete MVA pathway was reconstructed in the peroxisome to harvest the peroxisomal acetyl-CoA, an additional 40-fold increase in squalene production was observed, yielding 2.34 g/L in strain Sq10 (Sq10 vs. Sq09, Fig. 2*B*), which also showed 1.37-fold higher than that of strain

Downloaded from https://www.pnas.org by MASARYK UNIVERSITY KNIHOVNA UNIVERZITNIHO KAMPUSU on November 3, 2024 from IP address 147.251.22.2.

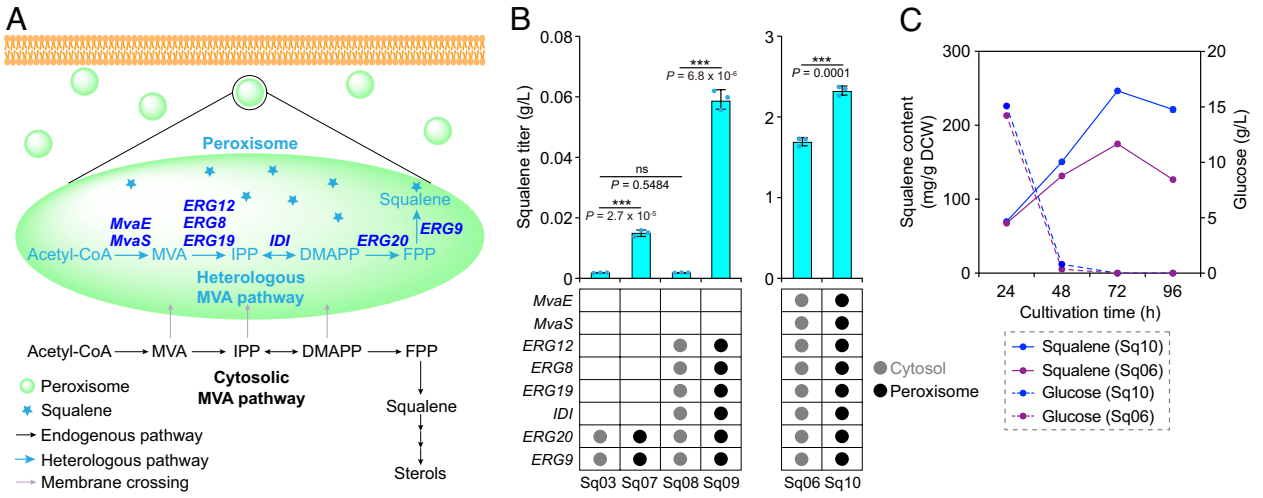

Fig. 2. Construction of the sequestered biosynthetic route for squalene in the peroxisome. (*A*) Schematic illustration of the orthogonal pathway for squalene production in the peroxisome. Conventional biosynthesis of squalene in *Y. lipolytica* relies on the endogenous cytosolic MVA pathway (shown in black), which tightly couples with sterol synthesis. Here, we build an orthogonal pathway for squalene synthesis in the peroxisome by introducing the complete squalene pathway starting from acetyl-CoA (shown in blue), in which the MVA pathway was assembled to harvest peroxisomal acetyl-CoA. (*B*) The entire squalene pathway was sequentially assembled in the peroxisome or overexpressed in the cytosol, respectively. Squalene titers were measured after 72 h of fermentation. (*C*) Time-course profiles of squalene content and glucose concentration in media of strain Sq06 overexpressing the cytosolic pathway and strain Sq10 harboring the peroxisomal pathway. Statistical significance was tested using the two-sided Student's *t* test; ***$P < 0.001$; ns, not significant. All data are represented as mean ± SD of three biologically independent experiments.

Sq06 overexpressing the MVA pathway in the cytosol (Sq10 vs. Sq06, Fig. 2*B*). These data clearly suggest that the heterologous MVA pathway is able to harvest the acetyl-CoA pool in the peroxisome for triterpene synthesis. It also confirmed that the entire squalene pathway when sequestered in the peroxisome could potentially eliminate the limitations imposed by competing cytosolic pathways for sterol synthesis. This was further confirmed by the time course of squalene concentration (Fig. 2*C*). During the initial 24 h, squalene concentration in strain Sq06 was similar to that of Sq10 harboring the squalene peroxisome pathway. However, after that, especially during glucose depletion (48 h to 72 h), squalene productivity in strain Sq06 gradually decreased (from 2.7 to 1.8 mg/g DCW/h), as, possibly, squalene formed in the cytosol was channeled to the sterol pathway, whereas strain Sq10 continued squalene build-up in the peroxisome with an elevated productivity (from 3.3 to 4.0 mg/g DCW/h).

To be noted, despite the 37% increase in squalene production in strain Sq10 over Sq06, the increase is small when compared to the fold change between Sq07 and Sq03 (6.3-fold) or Sq09 and Sq08 (24.4-fold) (Fig. 2*B*). This suggests that the acetyl-CoA supply in the peroxisome is insufficient and compromises the performance of the peroxisomal squalene pathway. Conversely, adequate acetyl-CoA pool in the cytosol may compensate for the loss of squalene for the sterol pathway, thus reducing the gap of squalene production between cytosolic engineered strain Sq06 and peroxisome engineered strain Sq10. As a result, the insufficient acetyl-CoA supply in the peroxisome becomes the bottleneck for further increasing squalene accumulation.

Converting Lipid By-Product to Peroxisomal Squalene. To cure a potential acetyl-CoA limitation, we next aimed to enhance the supply of this precursor in the peroxisome by engineering lipid metabolism, namely, lipid biosynthesis, hydrolysis, and degradation processes (Fig. 3*A*). *Y. lipolytica* is a natural lipid producer capable of accumulating lipid at 30 to 60% of dry cell weight (37), mainly in the form of triacylglycerols (TAGs) stored in lipid bodies. Similar to lipid bodies that facilitate lipophilic compound sequestration and storage, engineered peroxisomes can also serve as storage compartment for accumulating squalene locally formed. We hypothesized that the accumulated TAGs in lipid bodies would serve as carbon source to support additional peroxisomal squalene production. In this section, we describe our attempts to increase squalene precursor supply based on this hypothesis.

We first attempted to convert the intracellular TAGs to free fatty acids (FFAs) that are degraded via β-oxidation to generate acetyl-CoA in the peroxisome, by overexpressing either the endogenous lipases (ylTGLs)-mediated TAG hydrolysis or a heterologous tlTGL from *Thermomyces lanuginosus* (39) in peroxisomal squalene-producing strain Sq10 (Fig. 3*A*). Overexpression of ylTGLs improved squalene production only slightly (*SI Appendix*, Fig. S4), while the introduction of lipid body-targeted tlTGL significantly improved squalene titer by 12% (Sq14 vs. Sq10, Fig. 3*B*). This result suggested that intracellular, lipid body-stored, TAGs were funneled to peroxisomal squalene synthesis and contributed to high yield. Moreover, it suggested that there is still considerable capacity for improving peroxisomal squalene synthesis by converting acetyl-CoA pool in the cytosol to peroxisomal acetyl-CoA through lipid metabolism.

We next overexpressed the key enzymes involved in TAG synthesis, including acetyl-CoA carboxylase (ACC1) (40), which converts acetyl-CoA into malonyl-CoA (the first committed step of TAG synthesis), diacylglycerol acyltransferase (DGA1) (40) catalyzing the ultimate step in TAG synthesis, and NAD^+-dependent G3P dehydrogenase (GPD1) converting dihydroxyacetone phosphate (DHAP) into glycerol-3-phosphate (G3P) (41). As expected, their overexpression led to a significant increase in lipid content (Sq15 vs. Sq14, *SI Appendix*, Fig. S5). Correspondingly, the peroxisomal squalene production was also elevated considerably by 16% (Sq15 vs. Sq14, Fig. 3*B*), as result of the higher precursor flux through the peroxisomal pathway. We also investigated the effect on cytosolic pathway-based squalene production in strain Sq06 by overexpressing these three enzymes. A considerably lower squalene production was observed (Sq16 vs. Sq06, *SI Appendix*, Fig. S6*A*). One plausible explanation could be that in the competition between lipid and squalene synthesis in the cytosol, lipid

Downloaded from https://www.pnas.org by MASARYK UNIVERSITY KNIHOVNA UNIVERZITNIHO KAMPUSU on November 3, 2024 from IP address 147.251.22.2.

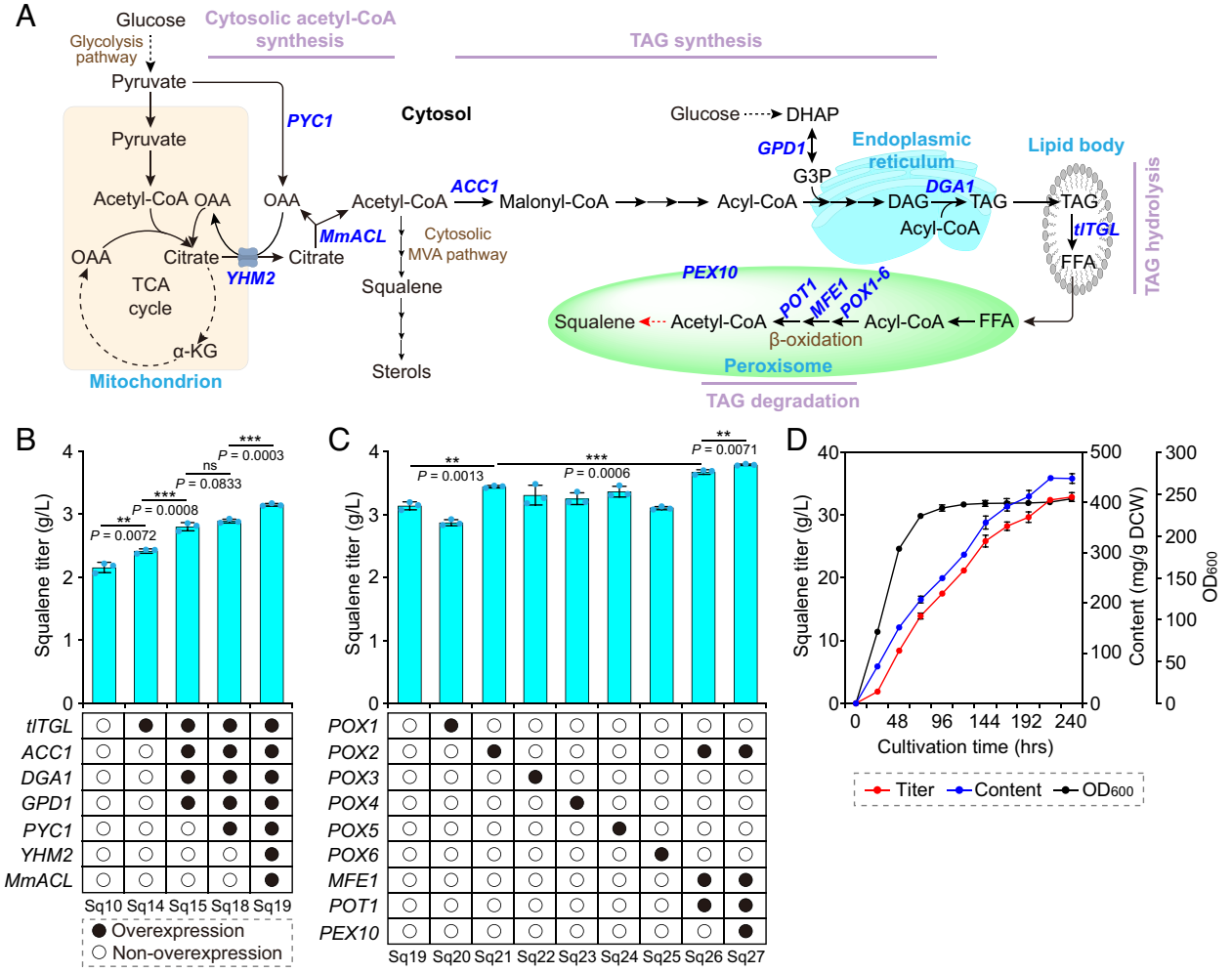

Fig. 3. Converting lipid by-product to peroxisomal squalene through lipid metabolism. (*A*) Schematic illustration of intracellular lipid metabolism, including its biosynthesis, hydrolysis, and degradation. Overexpressed genes in this study are shown in blue. PYC1, pyruvate carboxylase. YHM2, mitochondrial citrate carrier. MmACL, ATP:citrate lyase from *Mus musculus*. ACC1, acetyl-CoA carboxylase. GPD1, NAD^+-dependent G3P dehydrogenase. DGA1, diacylglycerol acyltransferase. tlTGL, lipase from *T. lanuginosus*. POX1-6, acyl-CoA oxidases. MFE1, multifunctional β-oxidation protein. POT1, 3-ketoacyl-CoA thiolase. PEX10, peroxisome biogenesis factor. (*B*) Engineering lipid biosynthesis and hydrolysis by overexpressing rate-limiting enzymes increased squalene production in the peroxisome. (*C*) Engineering lipid degradation by strengthening the β-oxidation pathway increased squalene production in the peroxisome. (*D*) Fermentation profiles of squalene-producing strain Sq27 in a 3-L bioreactor. Statistical significance was tested using the two-sided Student's *t* test; $^{**}P < 0.01$ and $^{***}P < 0.001$; ns, not significant. All data are represented as mean ± SD of three biologically independent experiments.

synthesis prevailed with more cytosolic acetyl-CoA channeled into lipid synthesis (*SI Appendix*, Fig. S6*B*), which, in turn, resulted in reduced flux into cytosolic MVA and squalene-forming pathway. While lipid bodies in *Y. lipolytica* generally supply hydrophobic pockets which facilitate the sequestration and storage for lipophilic terpenoids (42), enhanced TAG synthesis comes at the expense of the common precursor acetyl-CoA in the cytosol. Therefore, it is necessary to optimally partition carbon flux between lipid and terpenoid synthesis. Alternatively, construction of an orthogonal terpenoid pathway in the peroxisome efficiently circumvented this limitation. We also attempted to increase cofactor NADPH supply required for de novo lipid biosynthesis (43), by overexpressing two genes G6PD (encoding glucose-6-phosphate dehydrogenase) and 6PGD (encoding phosphor-gluconate dehydrogenase) involved in the pentose phosphate pathway. However, neither squalene nor lipid production improved significantly (*SI Appendix*, Fig. S7), suggesting that NADPH recycling is not the rate-limiting in this case. As a result, we did not further pursue this strategy.

Cytosolic acetyl-CoA is the main precursor for lipid and squalene synthesis. Since sufficient metabolic flux of cytosolic acetyl-CoA is critical for both lipid and squalene production, we tried to increase its supply. Pyruvate carboxylase (PYC1) was first overexpressed to ensure efficient formation of oxaloacetate required for citrate biosynthesis and transport (Fig. 3*A*). However, overexpressing PYC1 resulted in marginal increase in squalene production (Sq18 vs. Sq15, Fig. 3*B*). We found that the citrate concentration significantly increased upon PYC1 overexpression (*SI Appendix*, Fig. S8). Given citrate as critical intermediate involved in cytosolic acetyl-CoA formation (Fig. 3*A*), we thus attempted to maximize the decomposition of citrate to form acetyl-CoA and oxaloacetate catalyzed by ATP:citrate lyase (ACL). We next introduced a heterologous ACL from *Mus musculus* (MmACL) because of its higher affinity for citrate (K_m of 0.05 mM) than the endogenous ones (K_m of 3.6 mM) (44). Furthermore, the provision of cytosolic acetyl-CoA this way also relies on mitochondrial activity for citrate exportation. Therefore, we overexpressed MmACL together with YHM2, the *Y. lipolytica* mitochondrial citrate carrier that was characterized as an antiporter for citrate and α-ketoglutarate or oxaloacetate (45). This enhanced precursor acetyl-CoA supply for lipid and squalene synthesis and significantly increased squalene production by 8.6%, reaching 3.17 g/L in strain Sq19 (Sq19 vs. Sq18, Fig. 3*B*).

Downloaded from https://www.pnas.org by MASARYK UNIVERSITY KNIHOVNA UNIVERZITNIHO KAMPUSU on November 3, 2024 from IP address 147.251.22.2.

Although in the above strain carbon flux was apparently redirected to peroxisome promoting peroxisomal squalene synthesis (1.45-fold increase in Sq19 vs. Sq10, Fig. 3*B*), the accumulated lipid pool in strain Sq19 (*SI Appendix*, Fig. S5) suggested that lipid degradation into acetyl-CoA in the peroxisome might be limiting. We therefore attempted next to increase lipid-to-squalene yield through strengthening the β-oxidation pathway that drives acyl-CoA conversion to acetyl-CoA in the peroxisome (Fig. 3*A*). The peroxisome β-oxidation pathway in yeast is a multistep process requiring three different enzymatic activities (Fig. 3*A*), including six acyl-CoA oxidases encoded by six genes *POX1* to *POX6* (46), which are responsible for the first committed step of β-oxidation, Multifunctional β-oxidation protein (MFE1) involved in the second and third β-oxidation steps (47), and 3-ketoacyl-CoA thiolase (POT1) catalyzing the last step (48). To explore the possible rate-limiting steps in the β-oxidation pathway, the six acyl-CoA oxidases were first individually overexpressed in peroxisomal production strain Sq19. Of the six acyl-CoA oxidases, overexpressing POX2 exhibited the most significant improvement of squalene synthesis in strain Sq21 (Sq21 vs. Sq19, Fig. 3*C*), as POX2 preferentially oxidizes long-chain fatty acids (46) that are the most abundant in *Y. lipolytica*. Subsequently, additional co-overexpression of MFE1 and POT1 further resulted in 6.7% increase in squalene production (Sq26 vs. Sq21, Fig. 3*C*). In addition, the number of peroxisome organelles is another factor that may affect peroxisomal production, because of its potential capacity of increasing the space for enzyme expression and product storage. Thus, we investigated the effect of increased peroxisome population on peroxisomal squalene production by overexpressing the peroxisome biogenesis factor 10 (*PEX10*) that plays a role in regulating the size and/or number of peroxisomes (48). Pex10 overexpression further improved squalene production by 3.1 % and yielded 3.82 g/L in strain Sq27 (Sq27 vs. Sq26, Fig. 3*C*).

Taken together, all steps converting lipid by-product to peroxisomal acetyl-CoA pool led to a total increase of 63% in squalene production in the peroxisome (Sq27 vs. Sq10, Fig. 3 *B* and *C*). This suggests that engineering lipid metabolism can support the synthesis of acetyl-CoA-derived chemicals in the peroxisome. We finally evaluated the performance of strain Sq27 in 3-L fed-batch cultivation with glucose as carbon source. Final titers of 32.8 g/L and content of 446 mg/g DCW were obtained (Fig. 3*D*), with a productivity of 0.15 g/L/h. These data demonstrate the robustness of our engineered strains in the fermentation of scale-up and high-cell density.

Establishing An Orthogonal Acetyl-CoA Shortcut in the Peroxisome. We also explored other options to increase the supply of acetyl-CoA in the peroxisome that bypass the long pathway of lipid metabolism investigated in the previous section. It has been reported that *Y. lipolytica* harbors the active acetate utilization pathway, suggesting that acetate could serve as direct source of acetyl-CoA (37) (Fig. 4*A*). To capitalize on this property, we first investigated the effect of acetate on squalene production in strain Sq10 harboring the peroxisomal pathway by feeding 27.4 g/L sodium acetate as carbon source (equivalent to 20 g/L glucose), supplemented with 0.2 M PBS (pH 6.0) for pH control. We found that when strain Sq10 was cultured in YPA media (acetate as carbon source), its squalene accumulation was similar to that in YPD media (glucose as carbon source) without PBS supplementation, but was 40% lower than that obtained in YPD media with PBS supplementation (Fig. 4*B*). The lower squalene titer in YPA media may result from the reduced cell

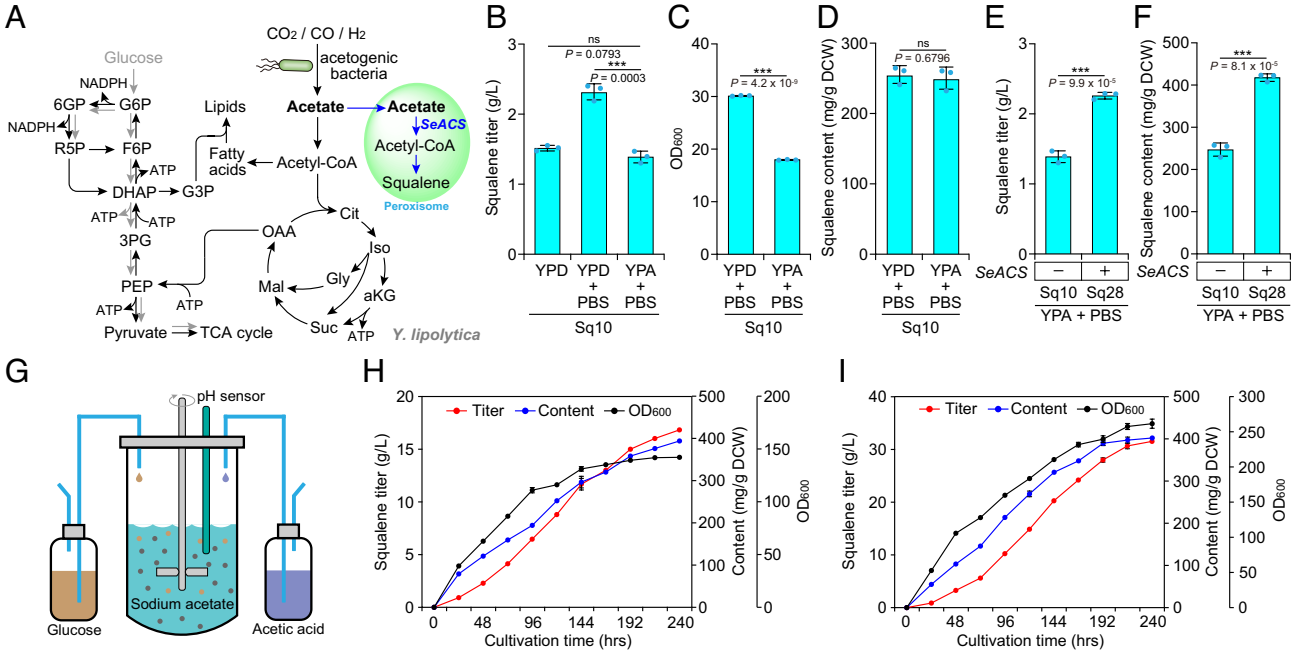

Fig. 4. Establishing an orthogonal acetyl-CoA shortcut in the peroxisome for squalene production. (*A*) Schematic illustration of the metabolic network based on acetate uptake. The blue arrows indicate the orthogonal squalene pathway starting from acetate in the peroxisome. The gray arrows indicate that the small fraction of glucose supplemented in substrate cofeeding system mainly support cell growth. SeACS, acetyl-CoA synthetase from *Salmonella enterica*. (*B*) Profiles of squalene production when stain Sq10 was grown in YPA media supplemented with PBS. (*C* and *D*) A decreased biomass was observed when strain Sq10 cultured in YPA media (*C*) relatively to that in YPD media, whereas squalene content in both YPA and YPD media is similar (*D*). (*E* and *F*) Introduction of SeACS (SeACS^{L641P}) in the peroxisome forming an orthogonal acetate utilization pathway in strain Sq28 increased significantly squalene production in terms of titers (*E*) and cellular content (*F*), compared to the parent strain Sq10. (*G*) Acetic acid in both salt and acid forms as carbon source was implemented in acetate fermentation in the bioreactor. In cofeeding glucose and acetate systems, glucose was continuously supplemented in small quantities to sustain a negligible concentration in the bioreactor and minimize catabolite repression. (*H* and *I*) Fermentation profiles of squalene-producing strain Sq28 on acetate-only culture (*H*) and on glucose-acetate mix cofeeding culture (*I*). Statistical significance was tested using the two-sided Student's *t* test; ***$P < 0.001$; ns, not significant. All data are represented as mean ± SD of three biologically independent experiments.

Downloaded from https://www.pnas.org by MASARYK UNIVERZITNIHO KAMPUSU on November 3, 2024 from IP address 147.251.22.2.

growth compared to that in YPD media (Fig. 4*C*), as squalene content was similar in both YPD and YPA media (Fig. 4*D*). This equivalent content demonstrates that *Y. lipolytica* can efficiently uptake acetate as carbon source to produce squalene.

Considering the nearly perfect performance of acetate as carbon source for squalene synthesis by harnessing the endogenous cytosolic acetate uptake pathway, we hypothesized that establishment of the orthogonal acetate utilization pathway in the peroxisome could potentially improve the peroxisomal acetyl-CoA pool and enhance acetate-to-squalene conversion. To this end, we introduced a heterologous acetyl-CoA synthetase variant (L641P, feedback inhibition-insensitive) from Salmonella enterica ($SeACS^{L641P}$) (49) and targeted its expression to the peroxisome. This created a metabolic shortcut to acetyl-CoA from acetate in the peroxisome for squalene synthesis (Fig. 4*A*). As a result, squalene titer was significantly increased by 63% (Sq28 vs. Sq10, Fig. 4*E*), as well as its elevated cellular content by 69% (Sq28 vs. Sq10, Fig. 4*F*), yielding 2.3 g/L and 420 mg/g DCW, respectively. We note that this orthogonal acetyl-CoA shortcut enabled strain Sq28 to produce a similar titer of squalene in YPA media, when compared to that of Sq10 in YPD media (Sq28 vs. Sq10, Fig. 4 *B* and *E*). We even observed that the cellular squalene content in strain Sq28 reached similar production level as prior strain Sq27 (obtained by the previous engineering approach) grown in YPD media (420 mg/g DCW in Sq28 vs. 424 mg/g DCW in Sq27). These results show that deploying the orthogonal acetate utilization pathway in the peroxisome allows one to bypass the long lipid metabolic steps and create a peroxisomal acetyl-CoA shortcut. Subsequently, our attempt to further increase acetyl-CoA by overexpressing POX2, MFE1, POT1, and PEX10 was not successful as only slight increase of squalene production was observed in terms of both titer and cellular content (Sq28 vs. Sq29, *SI Appendix*, Fig. S9). It is possible that the amount of acetyl-CoA derived from acetate in the peroxisome is sufficient for the present capacity of the downstream pathway of squalene synthesis. Finally, we investigated the performance of engineered strain Sq28 for squalene production in a scaled-up bioreactor. A joint feeding strategy was employed, where acetate was fed in both the salt and acid forms (Fig. 4*G*). The latter serves with the dual functions of carbon source as well as pH regulator. This strategy achieved 16.8 g/L of squalene with a cellular content of 394 mg/g DCW (Fig. 4*H*).

Relatively to growth on glucose, our results showed that the reduced amount of cell biomass when grown on acetate was the main reason for the reduced squalene titer. To remedy this, without additional genetic modulations, we implemented a cofeeding scheme of acetate and controlled amounts of glucose. It has been demonstrated that when grown on less desirable primary substrate relatively to glucose, cell growth and productivity can be significantly enhanced by cofeeding small amounts of the preferred (glucose) substrate along with the primary substrate (50). While the exact biochemical basis of this phenomenon is still under investigation, one hypothesis is that preferred substrates provide an easier catabolizable carbon-energy source that allows the cells to generate the necessary amounts of ATP required for their growth and maintenance, thus contributing to a more dense and robust culture. Care must be exercised in controlling the feeding rate of the preferred substrate to prevent catabolite repression and seizure of utilization of the primary substrate (acetate). In our case, this strategy was implemented by cofeeding glucose and acetate, in which limiting quantities of glucose were continuously added over the course of fermentation to acetate culture (Fig. 4*G*). The glucose feed rate was kept quite low to sustain a negligible concentration (undetectable level) in the bioreactor and minimize catabolite repression. By this strategy, cells simultaneously consumed acetate and glucose, with acetate remaining as primary carbon source. Under these conditions, acetate utilization metabolism dominated to provide acetyl-CoA precursor for squalene production in the peroxisome. We ultimately nearly doubled the squalene titer (31.6 g/L, Fig. 4*I*) relatively to acetate-only fermentation (16.8 g/L, Fig. 4*H*), while a similar cellular content of squalene (402 mg/g DCW in the cofeeding fermentation vs. 394 mg/g DCW in acetate-only fermentation) was obtained (Fig. 4 *H* and *I*). In particular, the rate of cell growth with substrate cofeeding was nearly twice as fast as that of the acetate-only control (0.327 DCW/h vs. 0.178 DCW/h). The rate of acetate uptake was enhanced by 25% with glucose doping, suggesting that controlled continuous feeding of a preferred substrate did not inhibit the consumption of the less favored substrate. These results demonstrate an alternative approach for the synthesis of terpenoids and other acetyl-CoA-derived products.

Discussion

Engineering microorganisms for the production of fuels and chemical products requires management of competing reactions that can convert pathway intermediates to metabolites other than the product of interest. Various strategies have been devised for the solution of this problem, most of which are based on inactivating one or more reactions of the competing pathways. This method, however, may not work if the competing reactions form metabolites critical for the survival of the microorganism. Years of evolution have led to regulatory mechanisms that prevent alteration of flux distributions that would be detrimental to the survival of the organism.

In this study, we chose *Y. lipolytica* as microbial host to investigate the possibility of shielding the production pathway and its intermediates from competing reactions by sequestering the pathway in an intracellular organelle. We selected the peroxisome as the organelle where to accumulate the target product such as squalene because the peroxisome is relatively not essential for the survival of yeast and it contains ample stores of the key precursor, acetyl-CoA, for product synthesis. Additionally, the supply of acetyl-CoA could be increased in the peroxisome by enhancing lipid degradation reactions that generate additional acetyl-CoA. By engineering the pathways responsible for lipid synthesis and degradation as well as squalene synthesis we succeeded in constructing a strain of *Y. lipolytica* capable of accumulating many-fold higher amounts of squalene than the control and strains accumulating squalene in the cytosol where it could be converted to sterol, a compound essential for cell viability.

The higher productivity and accumulation of peroxisomal squalene suggest that peroxisomes can serve as efficient barrier insulating locally formed products from competing cytosolic pathways. This transforms peroxisomes into microfactories for accumulation of products, like squalene, while avoiding any disruption of cell growth. Although similar peroxisome engineering strategies have been previously applied in the conventional model yeast *S. cerevisiae* (9, 35), the full potential of this strategy remains largely unexplored for biosynthesis of terpenoid and other products in the oleaginous yeast *Y. lipolytica*. In this regard, *Y. lipolytica* may be a better host strain to apply the described sequestration strategy due to its high capacity for lipid synthesis and concomitant ability to generate copious amounts of acetyl-CoA in the peroxisome. This inherent advantage would make *Y. lipolytica* a preferred alternative host for peroxisomal production over nonoleaginous yeast *S. cerevisiae*. This advantage is further accentuated by the fact that the above strategy allows for the recycle of carbon used for lipid synthesis toward terpenoid synthesis and thus minimizes concerns

Downloaded from https://www.pnas.org by MASARYK UNIVERSITY KNIHOVNA UNIVERZITNIHO KAMPUSU on November 3, 2024 from IP address 147.251.22.2.

of unwanted side product formation. Degradation of such products (i.e., lipids) and efficient recycle of the product acetyl-CoA for the synthesis of desired terpenoid products minimizes concerns of inefficient use of carbon precursors.

Construction of acetyl-CoA shortcut in the peroxisome through the acetate utilization pathway greatly simplified supply of precursor and avoided negative feedback regulations in host metabolism, relatively to the approach of converting acetyl-CoA pool in the cytosol to peroxisomal acetyl-CoA through the long pathway of lipid metabolism. The latter is facing to be inefficient in terms of ATP and NADPH costs. In light of this, introduction of acetate-utilizing route for precursor supply to the peroxisomal squalene pathway decoupled product synthesis from native metabolism, circumventing precursor/cofactor competitions and metabolic cross talks. Although acetate-only fermentation exhibited suboptimal cell growth, this problem was solved by substrate cofeeding strategy with small amounts of continuously supplied glucose. The efficient utilization of acetate for product synthesis presents the potential of employing acetic acid as low-cost feedstock for the production of acetyl-CoA-derived products. Acetic acid can be generated from biological CO_2 fixation, lignocellulosic biomass degradation, and industrial waste stream digestion (51). Therefore, usage of acetic acid as carbon source to produce biofuels and green chemicals would contribute toward achieving net-zero greenhouse gas emissions.

Materials and Methods

Strain Cultivation and Medium. *E. coli* DH5α were used for plasmid propagation. The *E. coli* strains harboring recombinant plasmid were grown in Luria-Bertani (LB) medium (Gibco) which was supplemented with 50 μg/mL kanamycin at 37 °C for 16 h. All *Yarrowia lipolytica* strains were cultured at 30 °C for 16 to 72 h. The *Y. lipolytica* strains were cultured in YPD medium which was prepared with 10 g/L yeast extract (VWR Life Science), 20 g/L peptone (VWR Life Science), and 20 g/L glucose (Sigma-Aldrich). 15 g/L agar (Sigma-Aldrich) was added for agar plates, if needed. YPA broth for squalene biosynthesis was prepared with 10 g/L yeast extract (VWR Life Science), 20 g/L peptone (VWR Life Science), and 27.4 g/L sodium acetate (Sigma-Aldrich). Phosphoric buffer solution (PBS) was prepared with 0.2 M Na_2HPO_4 and 0.2 M NaH_2PO_4 and was adjusted to pH 6.0, which was added to YPD or YPA medium for squalene production. YNB medium was prepared with 1.7 g/L yeast nitrogen base without amino acids and ammonium sulfate (YNB, BD bioscience), 20 g/L glucose (Sigma-Aldrich), 5 g/L ammonium sulfate (Sigma-Aldrich), and 15 g/L agar (Sigma-Aldrich), in which the complete amino acid supplement mixture without leucine, uracil, tryptophan, or lysine (Sunrise science products) was supplemented to select the transformed *Y. lipolytica* strains. Regarding antibiotic selection of *Y. lipolytica* strains, 250 μg/mL hygromycin B (Sigma-Aldrich) or 400 μg/mL nourseothricin (Fisher Scientific) was supplemented to YPD medium.

Plasmids and Strains. *E. coli* DH5α used for gene clone was purchased from New England Biolabs (NEB). *Y. lipolytica* base strain Po1f was stocked in the lab. The engineered *Y. lipolytica* strains and recombinant plasmids for in this work are shown in *SI Appendix*, Table S1. The primers for plasmid construction were synthesized in Sigma-Aldrich and are listed in *SI Appendix*, Table S2. The Not1 enzyme (NEB) was used to linearize plasmid for *Y. lipolytica* transformation. KAPA HiFi DNA polymerase purchased from Kapa Biosystems was used to amplify the target genes for the construction of plasmids. GoTaq DNA polymerase purchased from Promega was used for the identification of the colony PCR. The DNA Gel Extraction Kit purchased from NEB was used to purify the DNA PCR fragments. The NEBuilder HiFi DNA Assembly Master Mix (NEB) was used for plasmid construction, and the recombinant plasmids were then transformed into chemically competent *E. coli* DH5α cells by heat shock. The QIAprep Spin Miniprep Kit (Qiagen) was used to extract recombinant plasmids, and the latter was further confirmed by sequencing at Quintara Bioscience. The recombinant plasmids were subsequently linearized by Not1 enzyme and were introduced into *Y. lipolytica* by the approach of lithium acetate. The engineered strains were verified by colony PCR prior to fermentation. Heterologous genes MvaE (WP_002357755.1) and MvaS (WP_002357756.1) sourced from *E. faecalis*, lipase tlTGL (O59952.1) from *T. lanuginosus*, and acetyl-CoA synthetase SeACS (WP_000083869.1) from *Salmonella enterica* were codon optimized toward *Y. lipolytica* and were synthesized at Thermo Fisher Scientific.

LYS5 Disruption in *Y. lipolytica* Strains. Previously, we obtained a *Y. lipolytica* Po1f variant Po1f-T in which the TRP1 gene was disrupted using CRISPR-Cas9 technology, resulting in available three auxotrophic markers (ura3$^-$, leu2$^-$, and trp1$^-$) (36). To exploit more available auxotrophic markers, we here use a similar approach to disrupt LYS5 (YALI0E09306) on the base of Po1f-T. The gRNA (TCTGACAGGCAAGAAGTGGA) targeting to LYS5 gene was constructed to CRISPR-Cas9 plasmid harboring Ura3 auxotrophic marker, and the successful recombinant plasmid was then transformed into Po1f-T strain. The engineered strains with lysine auxotrophy, due to LYS5 disruption, were further screened on the plates of YNB-Ura and YNB-Ura-lys, respectively. Subsequently, the successful colonies were inoculated to YPD medium for cultivation until the CRISPR-Cas9 plasmid was completely removed. The resulting strain was name as po1f-T-L with genotype of *ura3*$^-$, *leu2*$^-$, *trp1*$^-$, and *lys5*$^-$.

Fermentations in the Shake Flask. Single colony of engineered strains was collected from the YNB plate and then inoculated into YPD medium for cultivation at 30 °C for 16 h. The overnight strains were subsequently transferred to 10 mL YPD or YPA medium in 50 mL shake flask with initial OD_{600} of 0.1, and continue to grow at 30 °C for 2 to 3 d with shaking at 220 rpm.

Fermentations in the Bioreactor. Fed-batch cultivations were carried out in a 3-L bioreactor (New Brunswick BioFlo 115 system). For glucose fermentation, it was initialed with 1 L medium which contains 50 g/L yeast extract, 100 g/L peptone, 100 g/L glucose, and 0.2 M PBS with pH 6.0. The seed culture of engineered strains was made by inoculating appropriate strains into YPD medium supplemented with PBS and growing at 30 °C/220 rpm for 18 h. Subsequently, the activated strains were transferred into the bioreactor with a starting OD_{600} of 1.5 to 2.0. The temperature in fermentation was set to 30 °C. The dissolved oxygen in the bioreactor was set to 20% controlled by an agitation cascade of 200 to 850 rpm in the growth phase (0 to 48 h). The rate for sparging air into the bioreactor was set to 2 vvm. When starting to feed medium, the agitation and aeration were, respectively, decreased to 600 rpm and 1 vvm. The pH in fermentation was keep at 6.8 by supplementing 5 M HCL or 5 M NaOH. Antifoam 204 (Sigma-Aldrich) was added, if needed, to prevent foam in the fermentation. The fed-batch was started at 48 h of fermentation with concentrated YPD medium which contains 100 g/L yeast extract, 100 g/L peptone, 500 g/L glucose, and 0.2 M PBS. For acetate fermentation, the initial fermentation was started with 1 L medium which contains 25 g/L yeast extract, 50 g/L peptone, 50 g/L sodium acetate, and 0.2 M PBS with pH 6.0. The seed cultures were prepared by inoculating appropriate strains into YPD medium supplemented with PBS for overnight growth, and then inoculated into YPA medium supplemented with PBS for extra 24-h cultivation, aiming at making the cells to adapt to acetate environment before inoculating seed culture into the bioreactor. The fed-batch process was initiated with feeding concentrated acetic acid (Sigma-Aldrich) as carbon source. The supplemented acetic acid also acts pH regulator to maintain pH at 6.8. The concentrated YP medium (100 g/L yeast extract and 100 g/L peptone) prepared with 0.2 M PBS was added to provide nitrogen source for cell growth. In substrate cofeeding systems, the added glucose was continuously fed at a quite slow rate to sustain its concentration in the bioreactor at an undetectable level. Samples were collected very 24 h to detect OD_{600}, glucose or acetate concentration, and squalene production.

Measurement of Glucose and Acetate in the Medium. Determination of glucose and acetate concentration in the medium was carried out through High-Performance Liquid Chromatography (HPLC, Agilent technologies 1260 Infinity) which was equipped with a refractive index detector and a BioRad HPX-87H column. The mobile phase was prepared with 14 mM sulfuric acid (Sigma-Aldrich) and flowed at the rate of 0.7 mL/min at 50 °C. The samples for injection into HPLC were prepared from the supernatant of culture, which were filtered by 0.2-μm syringe filters.

Lipid Extraction and Quantification. 0.5 mL cell culture was collected and centrifuged at 12,000 g for 2 min, and the supernatant was discarded. 0.5 mL solution of sodium hydroxide-methanol (0.5 M) was then added and resuspend the cell pellets, which was followed by adding the internal standards, including

Downloaded from https://www.pnas.org by MASARYK UNIVERSITY KNIHOVNA UNIVERZITNIHO KAMPUSU on November 3, 2024 from IP address 147.251.22.2.

methyl tridecanoate and glyceryl triheptadecanoate (2 mg/mL, Sigma-Aldrich). The mixture was vortexed for 1 h at room temperature, which could transesterify the lipids to fatty acid methyl esters (FAMEs). After that, 40 μL sulfuric acid (Sigma-Aldrich) was added for pH neutralization. Subsequently, 0.5 mL hexane (Sigma-Aldrich) was added and vortexed for 30 min to extract the FAMEs. The upper hexane phase was collected for analysis by a spin at 12,000 g for 2 min. Quantification of FAMEs was performed by GC-FID (Agilent technologies 7890B) which was equipped with an Agilent HP-INNOWAX capillary column. The process of GC oven temperature was as follows: initial temperature was set 100 °C, then ramped to 240 °C at a rate of 50 °C/min, held for 10 min. 1 μL sample was injected into GC with a split ratio of 50:1, and the inlet temperature was set to 260 °C. Fatty acids were identified and quantified by comparison with commercial FAME standards (Sigma-Aldrich). The total content of lipids was determined by the sum of five FAMEs below: methyl palmitate (C16:0), methyl palmitoleate (C16:1), methyl stearate (C18:0), methyl oleate (C18:1), and methyl linoleate (C18:2).

Extraction and Quantification of Squalene. 100 to 500 μL cell culture was collected and centrifuged at 12,000 g for 2 min. Cell pellets were then suspended in 500 μL methanol with glass beads (425 to 600 μm, Sigma-Aldrich). The cell mixture was then vortexed for 60 min at room temperature. After that, 500 μL hexane was added and vortexed for extra 30 min. The upper hexane phase was collected for analysis by centrifugating at 12,000 g for 5 min. Quantification of squalene was performed by GC-FID (Agilent technologies 7890B) which was equipped with an Agilent HP-INNOWAX capillary column. The process of GC oven temperature was as follows: initial temperature was set 100 °C for 0.5 min, then ramped to 250 °C at a rate of 50 °C/min, held for 8 min. 1 μL sample was injected into GC with a split ratio of 2:1, and the inlet temperature was set to 260 °C. Squalene was identified and quantified by comparison with commercial squalene standard (Sigma-Aldrich).

Data, Materials, and Software Availability. All study data are included in the article and/or *SI Appendix*.

ACKNOWLEDGMENTS. This work was funded by the National Key Research and Development Program of China (2018YFA0901800), the US Department of Energy (Grant number DE-SCOO22016), and Yunnan Science Fund (202105AF150028 and YSZJGZZ-2022091).

Author affiliations: [a]Department of Chemical Engineering, Massachusetts Institute of Technology, Cambridge, MA 02142; [b]Yunnan Key Laboratory of Potato Biology, Chinese Academy of Agricultural Sciences (CAAS)-Yunnan Normal University (YNNU)-YINMORE Joint Academy of Potato Sciences, Yunnan Normal University, Kunming 650500, China; and [c]Engineering Research Center of Sustainable Development and Utilization of Biomass Energy (Ministry of Education), Yunnan Normal University, Kunming 650500, China

1. Y. Chen, J. Nielsen, Advances in metabolic pathway and strain engineering paving the way for sustainable production of chemical building blocks. *Curr. Opin. Biotechnol.* **24**, 965–972 (2013).
2. P. P. Peralta-Yahya, F. Zhang, S. B. Del Cardayre, J. D. Keasling, Microbial engineering for the production of advanced biofuels. *Nature* **488**, 320–328 (2012).
3. Y. Liu, J. Nielsen, Recent trends in metabolic engineering of microbial chemical factories. *Curr. Opin. Biotechnol.* **60**, 188–197 (2019).
4. C. E. Vickers, T. C. Williams, B. Peng, J. Cherry, Recent advances in synthetic biology for engineering isoprenoid production in yeast. *Curr. Opin. Chem. Biol.* **40**, 47–56 (2017).
5. J. Nielsen, J. D. Keasling, Engineering cellular metabolism. *Cell* **164**, 1185–1197 (2016).
6. L. Dong *et al.*, Co-expression of squalene epoxidases with triterpene cyclases boosts production of triterpenoids in plants and yeast. *Metab. Eng.* **49**, 1–12 (2018).
7. D.-K. Ro *et al.*, Production of the antimalarial drug precursor artemisinic acid in engineered yeast. *Nature* **440**, 940–943 (2006).
8. C. J. Paddon *et al.*, High-level semi-synthetic production of the potent antimalarial artemisinin. *Nature* **496**, 528–532 (2013).
9. G.-S. Liu *et al.*, The yeast peroxisome: A dynamic storage depot and subcellular factory for squalene overproduction. *Metab. Eng.* **57**, 151–161 (2020).
10. C. Ignea *et al.*, Orthogonal monoterpenoid biosynthesis in yeast constructed on an isomeric substrate. *Nat. Commun.* **10**, 3799 (2019).
11. A. Chou, S. H. Lee, F. Zhu, J. M. Clomburg, R. Gonzalez, An orthogonal metabolic framework for one-carbon utilization. *Nat. Metab.* **3**, 1385–1399 (2021).
12. R. Thimmappa, K. Geisler, T. Louveau, P. O'Maille, A. Osbourn, Triterpene biosynthesis in plants. *Annu. Rev. Plant Biol.* **65**, 225–257 (2014).
13. J. D. Connolly, R. A. Hill, Triterpenoids. *Nat. Prod. Rep.* **27**, 79–132 (2010).
14. K. Paramasivan, S. Mutturi, Recent advances in the microbial production of squalene. *World J. Microbiol. Biotechnol.* **38**, 1–21 (2022).
15. M. Tateno *et al.*, Synthetic Biology-derived triterpenes as efficacious immunomodulating adjuvants. *Sci. Rep.* **10**, 1–11 (2020).
16. N. Gohil, G. Bhattacharjee, K. Khambhati, D. Braddick, V. Singh, Engineering strategies in microorganisms for the enhanced production of squalene: Advances, challenges and opportunities. *Front. Bioeng. Biotechnol.* **7**, 50 (2019).
17. Z.-T. Zhu *et al.*, Metabolic compartmentalization in yeast mitochondria: Burden and solution for squalene overproduction. *Metab. Eng.* **68**, 232–245 (2021).
18. L. J. Wei *et al.*, Improved squalene production through increasing lipid contents in Saccharomyces cerevisiae. *Biotechnol. Bioeng.* **115**, 1793–1800 (2018).
19. A. Rasool, M. S. Ahmed, C. Li, Overproduction of squalene synergistically downregulates ethanol production in Saccharomyces cerevisiae. *Chem. Eng. Sci.* **152**, 370–380 (2016).
20. J. Y. Han, S. H. Seo, J. M. Song, H. Lee, E.-S. Choi, High-level recombinant production of squalene using selected Saccharomyces cerevisiae strains. *J. Ind. Microbiol. Biotechnol.* **45**, 239–251 (2018).
21. C. Zhou *et al.*, Engineering of cis-element in Saccharomyces cerevisiae for efficient accumulation of value-added compound squalene via downregulation of the downstream metabolic flux. *J. Agric. Food. Chem.* **69**, 12474–12484 (2021).
22. T. Li *et al.*, Metabolic engineering of Saccharomyces cerevisiae to overproduce squalene. *J. Agric. Food. Chem.* **68**, 2132–2138 (2020).
23. K. Paramasivan, P. K. HN, S. Mutturi, Systems-based Saccharomyces cerevisiaes strain design for improved squalene synthesis. *Biochem. Eng. J.* **148**, 37–45 (2019).
24. K. Paramasivan, N. Gupta, S. Mutturi, Adaptive evolution of engineered yeast for squalene production improvement and its genome-wide analysis. *Yeast* **38**, 424–437 (2021).
25. W. Xu *et al.*, Improving squalene production by enhancing the NADPH/NADP+ ratio, modifying the isoprenoid-feeding module and blocking the menaquinone pathway in *Escherichia coli*. *Biotechnol. Biofuels* **12**, 1–9 (2019).
26. J.-J. Pan *et al.*, Biosynthesis of squalene from farnesyl diphosphate in bacteria: Three steps catalyzed by three enzymes. *ACS Central Sci.* **1**, 77–82 (2015).
27. A. Katabami *et al.*, Production of squalene by squalene synthases and their truncated mutants in Escherichia coli. *J. Biosci. Bioeng.* **119**, 165–171 (2015).
28. Y. Meng *et al.*, Extension of cell membrane boosting squalene production in the engineered Escherichia coli. *Biotechnol. Bioeng.* **117**, 3499–3507 (2020).
29. S. Gao *et al.*, Iterative integration of multiple-copy pathway genes in Yarrowia lipolytica for heterologous β-carotene production. *Metab. Eng.* **41**, 192–201 (2017).
30. Y.-Y. Huang *et al.*, Enhanced squalene biosynthesis in Yarrowia lipolytica based on metabolically engineered acetyl-CoA metabolism. *J. Biotechnol.* **281**, 106–114 (2018).
31. L.-J. Wei *et al.*, Increased accumulation of squalene in engineered Yarrowia lipolytica through deletion of PEX10 and URE2. *Appl. Environ. Microbiol.* **87**, e00481-00421 (2021).
32. W.-Y. Tang *et al.*, Metabolic engineering of Yarrowia lipolytica for improving squalene production. *Bioresour. Technol.* **323**, 124652 (2021).
33. H. Liu, F. Wang, L. Deng, P. Xu, Genetic and bioprocess engineering to improve squalene production in Yarrowia lipolytica. *Bioresour. Technol.* **317**, 123991 (2020).
34. X. Luo *et al.*, Complete biosynthesis of cannabinoids and their unnatural analogues in yeast. *Nature* **567**, 123–126 (2019).
35. S. Dusséaux, W. T. Wajn, Y. Liu, C. Ignea, S. C. Kampranis, Transforming yeast peroxisomes into microfactories for the efficient production of high-value isoprenoids. *Proc. Natl. Acad. Sci. U.S.A.* **117**, 31789–31799 (2020).
36. Y. Ma *et al.*, Removal of lycopene substrate inhibition enables high carotenoid productivity in Yarrowia lipolytica. *Nat. Commun.* **13**, 572 (2022).
37. H. Liu, M. Marsafari, F. Wang, L. Deng, P. Xu, Engineering acetyl-CoA metabolic shortcut for eco-friendly production of polyketides triacetic acid lactone in Yarrowia lipolytica. *Metab. Eng.* **56**, 60–68 (2019).
38. A. A. Sibirny, Yeast peroxisomes: Structure, functions and biotechnological opportunities. *FEMS Yeast Res.* **16**, fow038 (2016).
39. K. Yang *et al.*, Subcellular engineering of lipase dependent pathways directed towards lipid related organelles for highly effectively compartmentalized biosynthesis of triacylglycerol derived products in Yarrowia lipolytica. *Metab. Eng.* **55**, 231–238 (2019).
40. M. Tai, G. Stephanopoulos, Engineering the push and pull of lipid biosynthesis in oleaginous yeast Yarrowia lipolytica for biofuel production. *Metab. Eng.* **15**, 1–9 (2013).
41. T. Dulermo, J.-M. Nicaud, Involvement of the G3P shuttle and β-oxidation pathway in the control of TAG synthesis and lipid accumulation in Yarrowia lipolytica. *Metab. Eng.* **13**, 482–491 (2011).
42. M. Larroude *et al.*, A synthetic biology approach to transform Yarrowia lipolytica into a competitive biotechnological producer of β-carotene. *Biotechnol. Bioeng.* **115**, 464–472 (2018).
43. K. Qiao, T. M. Wasylenko, K. Zhou, P. Xu, G. Stephanopoulos, Lipid production in Yarrowia lipolytica is maximized by engineering cytosolic redox metabolism. *Nat. Biotechnol.* **35**, 173 (2017).
44. H. Zhang *et al.*, Enhanced lipid accumulation in the yeast Yarrowia lipolytica by over-expression of ATP: Citrate lyase from Mus musculus. *J. Biotechnol.* **192**, 78–84 (2014).
45. E. Y. Yuzbasheva *et al.*, The mitochondrial citrate carrier in Yarrowia lipolytica: Its identification, characterization and functional significance for the production of citric acid. *Metab. Eng.* **54**, 264–274 (2019).
46. A. Beopoulos *et al.*, Control of lipid accumulation in the yeast Yarrowia lipolytica. *Appl. Environ. Microbiol.* **74**, 7779–7789 (2008).
47. P. Kasaragod *et al.*, Structural enzymology comparisons of multifunctional enzyme, type-1 (MFE 1): The flexibility of its dehydrogenase part. *FEBS Open bio* **7**, 1830–1842 (2017).
48. J. J. Smith, T. W. Brown, G. A. Eitzen, R. A. Rachubinski, Regulation of peroxisome size and number by fatty acid β-oxidation in the yeast Yarrowia lipolytica. *J. Biol. Chem.* **275**, 20168–20178 (2000).
49. V. J. Starai, J. G. Gardner, J. C. Escalante-Semerena, Residue Leu-641 of acetyl-CoA synthetase is critical for the acetylation of residue Lys-609 by the protein acetyltransferase enzyme of Salmonella enterica. *J. Biol. Chem.* **280**, 26200–26205 (2005).
50. J. O. Park *et al.*, Synergistic substrate cofeeding stimulates reductive metabolism. *Nat. Metab.* **1**, 643–651 (2019).
51. J. Xu, N. Liu, K. Qiao, S. Vogg, G. Stephanopoulos, Application of metabolic controls for the maximization of lipid production in semicontinuous fermentation. *Proc. Natl. Acad. Sci. U.S.A.* **114**, E5308–E5316 (2017).

Downloaded from https://www.pnas.org by MASARYK UNIVERSITY KNIHOVNA UNIVERZITNIHO KAMPUSU on November 3, 2024 from IP address 147.251.22.2.